Study on energy consumption and thermal comfort performance of geothermal-powered underfloor heating systems

Amir Omidvar
Department of Mechanical & Aerospace Engineering
Shiraz University of Technology
Shiraz, Iran
omidvar@sutech.ac.ir

Hossein Taghvaei
School of Mechanical Engineering
Shiraz University
Shiraz, Iran

Hamed Taghvaei
School of Chemistry and Petroleum Engineering
Shiraz University
Shiraz, Iran

***Abstract*— Geothermal heating systems are energy efficient, long life, low maintenance and environmentally friendly. The greatest disadvantage of these systems would be the high initial cost of installation. Much of this cost is related to underground loop field (well drilling/excavating and tubing). The size of underground loop and consequently loop pricing depends on the building heating energy demand. Previous studies have found, radiant heating is more energy efficient than forced air systems. So, it seems that by combining radiant hydronic floor heating with ground source heat pumps, we can reduce the required borehole size and installation cost of geothermal heating systems. In the present study, thermal performance of the geothermal radiant floor heating (GRFH) was compared to conventional geothermal forced air (GFA) systems in buildings with various use and occupancy. Results indicated that, by using a GRFH system in heating dominated climates, the underground loop size can be reduced significantly. It was shown that the heat pump compressor work and the required borehole length for a GRFH system are about 12-18% and 20-27% lower compared to GFA systems in residential and official buildings, respectively.**

Keywords—Borehole length; Geothermal; Floor heating; Heat pump

I. INTRODUCTION

The constraints of resources and undesirable effects resulting from excessive consumption of energy resources in recent years, have led to the optimization of energy consumption and use of renewable energy resources [1]. In most countries, nearly 40% of energy is consumed in building section. So the use of renewable energy resources for heating and cooling of buildings is of particular importance [2]. Ground source heat pumps (GSHPs) are one of the instruments that have recently attracted much attention [3] which use the earth as a heat source (in winter) or a heat sink (in summer) [4]. These systems are energy efficient, long life, low maintenance and environmentally friendly. Temperature fluctuations of the earth is very small during the year and the ground takes very little impact from ambient temperature fluctuations; so it can be used as a suitable source/sink for heat pumps [4]. Ground heat exchangers (GHEs) with different configurations of tubes (vertical, horizontal and spiral) are used to extract heat from the ground or reject heat to the ground in GSHPs [5].

Several theoretical and experimental studies have been performed on GSHPs to investigate the performance of these systems [6-15]. Michopoulos and Kyriakis [6] studied the effect of vertical GHE length on the electricity consumption of the heat pumps. They used an analytical model to determine the required GHE length and simulated the operation of the system over a long period of time (e.g. 20 years). The input parameters in their model were the cooling and heating loads of the building, thermophysical properties of the borehole and the characteristic curves of the heat pump and the outputs were the electricity consumption and the amount of heat absorbed from or rejected to the ground. Casasso and Sethi [7] studied the efficiency of closed loop GSHPs and showed that the GHE length has the biggest effect on the performance of GSHPs. It was shown that further improvements can be obtained by using pipe spacers and high conductive grouts. Michopoulos and Kyriakis [8] proposed a model to predict the fluid temperature at the exit of the vertical GHE. The energy analysis GSHPs is based on the instantaneous fluid temperature at the GHE outlet because this temperature defines the coefficient of performance (*COP*) of the heat pump and hence the electricity consumption of it. Their model predicts the fluid temperature at the exit of the GHE based on the heat transfer in the soil and the temporal variations of the thermal load of the GHE. Lohani and Schmitdt [9] studied the energy and exergy analysis of three systems for heating the buildings: fossil plant, air source heat pump and GSHP. The results showed that the GSHP system is better than two other systems in terms of both the energy and exergy analysis. Also it was shown that the *COP* and the second law efficiency of the GSHP is 50% higher than the fossil plant and the GSHP has 25% less demand of absolute primary energy and exergy than the fossil plant. Zhai et al. [10] reviewed the applications and integrated approaches of GSHPs and showed that the proper integrated approaches of GSHPs will result in a *COP* of 3 to 5 for heat pumps. Also the hybrid systems showed a great potential to yield a payback of about 2-5 years compared to the conventional air conditioning systems. Lubis et al. [11] studied the thermodynamic analysis of a hybrid GSHP system using a cooling tower as supplemental heat rejecter and showed that the *COP* and second law efficiency of the system are 5.34 and 63.4% respectively. The *COP* of air source heat pumps is often between 1 and 3 and the second law efficiency of them is below 30% [12-15].

Conventional geothermal forced air (GFA) systems often use forced convective air distributors such as fan-coil or air handling units. Non-uniform distribution of heat in the room is one of the main defects of these systems. Forced air systems also can distribute allergens in the room that this is not desirable especially for the people with allergies. To overcome these drawbacks use of radiant floor heating systems can be useful. Radiant systems are noiseless and can provide high level of thermal comfort and air quality.

There are generally three types of radiant heating systems: radiant heating with warm air, warm water and electricity. The radiant heating systems which use warm water for heating are called hydronic systems. Hydronic floor heating systems have several attributes such as energy saving potential and ability to tie-in with moderate temperature and low intensity energy sources like solar and heat pumps [16]. Several theoretical and experimental studies have been performed to investigate the performance of radiant floor heating systems [17-21]. Rahimi and Sabernaeemi [17] experimentally investigated the radiation and free convection mechanisms in an enclosure with floor heating system and showed that the radiation is the main mechanism of heat transfer from the floor to other surfaces. They indicated that 75-80% of heat transfer is by radiation and the else by free convection. Zhang et al. [18] studied experimental and numerical analysis on the lightweight floor heating systems. The percentage of radiation mechanism has been reported 60% in steady state conditions. Fontana [19] experimentally investigated the performance of floor heating systems in furnished enclosures and showed that the existence of furniture in the room decreases the air temperature and the mean radiant temperature. Bojic et al. [20] studied the performance of different radiant heating systems: radiant floor, ceiling, walls and combined floor-ceiling. It was shown that the combined floor-ceiling heating system has the best performance, lowest energy consumption, lowest CO_2 emission and also lowest operational cost. Rahimi and Sabernaeemi [21] experimentally investigated the participation of radiation and free convection in an enclosure with radiant ceiling heating system. They showed that nearly 90% of the heat is transferred by radiation.

Radiant heating is more energy efficient than forced air systems. So, it seems that, we can improve the performance of conventional geo-exchange heating systems by combining ground source heat pumps with radiant underfloor heating. Radiant floor heating systems provide high level of thermal comfort and indoor air quality at low energy consumption. Also, by this combination we can reduce the size of the underground tubing network and consequently the installation cost of geothermal heating. The operating cost and CO_2 emissions of low temperature radiant heating panel systems using different heat sources (natural gas boiler, ground source heat pump and ground source heat pump with photovoltaic array to drive the compressor) have been compared in [22]. Results showed that newly developed floor-ceiling panel with GSHP+PV has the best performance.

Present study theoretically investigates energy consumption and the required borehole size of geothermal radiant floor heating systems.

II. METHODOLOGY

Current paper investigates the performance of the combined GSHP and hydronic floor heating system in terms of energy consumption and thermal comfort. For this purpose, modeling of different parts of the system has been considered and then coupling of models and the solution process have been performed. The schematic diagram of the proposed system can be seen in Fig.1. The simulation includes the modeling of heat transfer mechanisms in radiant floor heating system, modeling of the thermal comfort for occupants, modeling of the GHE and finally modeling of the heat pump.

A. *Modeling of Floor Heating System*

In a floor heating system, heat transfers by all three mechanisms of radiation, convection and conduction. Heat transfers by radiation from warm floor to other surfaces of room and warms them up.

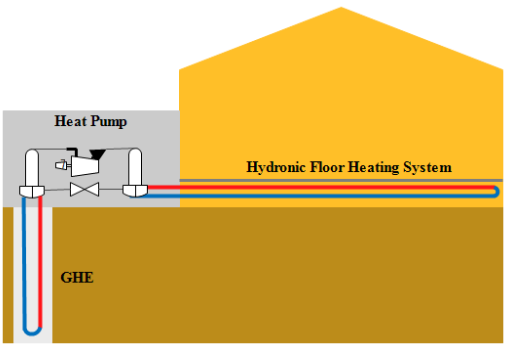

Fig. 1. *Schematic of a geothermal powered floor heating system*

The walls, floor and ceiling surfaces transfer heat to the air by free convection. Also a portion of heat in the room can transfer through walls and roof to outside by conduction. Energy balance equations for walls, floor, ceiling and air should be written separately and the resulting system of equations should be solved to find the temperatures of each part. The energy balance equations for an enclosure with a radiant floor heating system are as follows. Energy balance equations for 4 lateral walls and the ceiling can be written as [23]:

$$\frac{(T_i-T_{out})A_i}{\left(R_{w,i}+\frac{1}{h_{out}}\right)} = h_{in}A_i(T_a-T_i)+\varepsilon(\sigma A_i)\times\left\{\sum_{j=1}^{6}F_{ij}\left(T_j^4-T_i^4\right)\right\} \quad (1)$$

It is assumed that the inside surfaces of room are single temperature Gray-Diffuse surfaces. Convective heat transfer coefficients are functions of surface temperature and can be calculated by the following equations [24].

$$h_{in}=\begin{cases}1.31(T_s-T_a)^{0.333} & Vertical\ surfaces\\ 1.52(T_s-T_a)^{0.333} & Horizontal\ surfaces\end{cases} \quad (2)$$

In a floor heating system, the heat source is in the floor so the energy balance equation for the floor in steady state conditions is [23]:

$$h_{in}\left(T_a-T_f\right)+\varepsilon\sigma\sum_{j=1}^{6}F_{fj}\left(T_j^4-T_f^4\right)+Q=0 \quad (3)$$

where, Q is the heat flux produced by the radiant heating panel. It is assumed that all of the heat loss of working fluid in the radiant panel is transferred from the floor to the room and there is no heat loss to the ground below the floor.

The energy balance for the air can be written as [23]:

$$\sum_{j=1}^{6}h_{in}(T_i-T_a)=\dot{m}_{inf}C_{p,a}\left(T_a-T_{inf}\right) \quad (4)$$

where, T_{inf} is the temperature of infiltrated air to the room and is usually considered equal to the outside air temperature. $\dot{m}_{inf}$ is the mass flow rate of infiltrated air to the room and is calculated from the following equation:

$$\dot{m}_{inf}=\rho\dot{V}=\rho\frac{ACH\times V}{3600} \quad (5)$$

where ACH is air change rate. So far, the energy balance equations for 6 internal surfaces of the room and also the air have been written; so a system of 7 nonlinear equations and 7 unknowns has been obtained. The temperatures of internal surfaces and the air are unknowns which can be calculated by solving the system of equations with simple iterative update of coefficients technique.

B. Thermal Comfort Model

Fanger [25] has presented the following equation to predict the thermal sensation of occupants in a room:

$$PMV = (303e^{-0.036M}+0.028)\{(M-W)-0.00305[5733-6.99(M-W)-P_a]-0.42[(M-W)-58.15]-1.7\times10^{-5}\times M(5867-P_a)-0.0014M(34-T_a)-3.96\times10^{-8}\times f_{cl}[(T_{cl}+273)^4-(T_{mrt}+273)^4]-f_{cl}h_{conv}(T_{cl}-T_a)\} \quad (6)$$

where, *M* and *W* are the metabolic rate and mechanical work in W/m^2 respectively. P_a and T_a are vapor partial pressure and temperature of the air. T_{cl} is the cloth temperature in °C and can be calculated from the following equation [26]:

$$T_{cl}=35.5-0.028(M-W)-0.155I_{cl}\{3.96\times10^{-8}\times f_{cl}[(T_{cl}+273)^4-(T_{mrt}+273)^4]+f_{cl}h_{conv}(T_{cl}-T_a)\} \quad (7)$$

h_{conv} is the convective heat transfer coefficient in W/m^{2}K and is calculated from Eq. (8) [25].

$$h_{conv}=\begin{cases}2.38(T_{cl}-T_a)^{0.25}\ ; & v<0.1\ \ m/s\\ 12.1\sqrt{v}\ ; & v>0.1\ \ m/s\end{cases} \quad (8)$$

The clothing factor (f_{cl}) can also be calculated from the following equation [24]:

$$f_{cl}=\begin{cases}1.0+0.2I_{cl} & ,I_{cl}<0.5\ clo\\ 1.05+0.11I_{cl} & ,I_{cl}>0.5\ clo\end{cases} \quad (9)$$

and, the mean radiant temperature (T_{mrt}) is calculated from [25]:

$$T_{mrt}=\sqrt[4]{T_1^4F_{p-1}+T_2^4F_{p-2}+\cdots+T_6^4F_{p-6}} \quad (10)$$

where T_1 to T_N are the absolute temperatures of surfaces in K and F_{p-1} to F_{P-6} are the radiation shape factors between the human body and each surface which can be calculated using the charts presented in [26].

The value of thermal comfort index *PMV* is an estimation of the expected average vote of a panel of evaluators for a given thermal environment. The thermal sensation index that has been adopted by Fanger is based on the seven-point psychophysical scale and is shown in Table 1 [25].

ISO standard 7730 recommends an interval of $-0.5\leq PMV\leq+0.5$ for thermal comfort [27]. If the floor is too warm or too cool, the occupants could feel uncomfortable owing to thermal sensation of their feet [27]. The local thermal discomfort caused by warm or cold floors can be estimated by the index of *PD* (percentage of dissatisfied) from the following equation [27]:

$$PD = 59.5022 - 74.6871 \times T_f + 16.4158 \times (T_f + 9.3362)\ln(T_f) \quad (11)$$

where, T_f is the floor temperature in °C. ISO Standard 7730 recommends a floor temperature range of 19–26 ˚C for light, mainly sedentary activity in winter and floor heating system design temperature of 29 ˚C [27]. The recommended temperature range for a carpeted floor is 21–28 ˚C giving an expected percentage of dissatisfied of 15% [27].

TABLE I. THERMAL SENSATION INDEX ADOPTED BY FANGER [25]

COLD	COOL	SLIGHTLY COOL	NEUTRAL	SLIGHTLY WARM	WARM	HOT
-3	-2	-1	0	1	2	3

C. Ground Heat Exchanger (GHE) Model

In a GSHP, heat is extracted from the ground via a borehole heat exchanger. Boreholes often consist of a U-tube which is surrounded by grout. Fig.2 shows schematic representation of a single borehole. For single family buildings it is normally enough to use one borehole but for larger heat demands, several boreholes can be connected [28]. The depth of boreholes varies from 60 to 250 m and depends on several parameters such as heat load, soil type and natural temperature in the ground etc. [28]. Philippe and Bernier [29] have presented the following equation to estimate the total length of a borehole for a given building:

$$L = \frac{q_h R_b + q_y R_{10y} + q_m R_{1m} + q_h R_{6h}}{T_{mean} - (T_{g0} + T_p)} \quad (12)$$

where, L is the total borehole length, T_{mean} is the mean fluid temperature in the borehole, T_{g0} is the undistributed ground temperature which is considered equal to the yearly average air temperature and T_p is the temperature penalty which represents a correction to the undistributed ground temperature due to thermal interferences between boreholes (in the case of a single borehole, T_p = 0). Eq. (12) is derived by the assumption that the heat transfer in the ground is only by conduction and the effects of moisture evaporation and underground water movement have not taken into account.

q_y, q_m and q_h represent the yearly average ground heat load, the highest monthly ground load and the peak hourly ground load, respectively. The amplitudes of these pulses are determined from the building load profile and the *COP* of the heat pump. The monthly and yearly pulses can be estimated using hourly simulation results or equivalent full load operating hours. Using the last method it is estimated that during the peak month, the heat pump operates half the time, so the monthly ground load is half of the peak hourly load. On the annual basis the net amount of heat absorbed from the ground or rejected to the ground is equivalent to a heat pump operating one-eighth of the time, which corresponds to one-eighth of the peak hourly ground load.

R_{10y}, R_{1m} and R_{6h} are effective ground thermal resistances corresponding to 10 years, one month and six hours ground loads. The effective ground thermal resistances account for transient heat transfer from the borehole wall to the far-field undistributed ground temperature. Calculations of effective ground thermal resistances are based on the infinite cylindrical source (ICS) solution and are expressed as follows:

$$R_{6h} = \frac{1}{k} G(\alpha\, t_{6h}/r_b^2) \quad (13)$$

$$R_{1m} = \frac{1}{k}[G(\alpha\, t_{1m+6h}/r_b^2) - G(\alpha\, t_{6h}/r_b^2)] \quad (14)$$

$$R_{10y} = \frac{1}{k}\left[G\left(\alpha\, t_{10y+1m+6h}/r_b^2\right) - G\left(\alpha\, t_{1m+6h}/r_b^2\right)\right] \quad (15)$$

where, *G*-function represents the cylindrical heat source solution. Philippe and Bernier [29] have presented simple curve fitted relations to calculate the *G*-function precisely.

R_b in Eq. (12) is the effective borehole thermal resistance and is the summation of the convective resistance of fluid in the borehole, the conduction resistance of tubes and the conduction resistance of grout which are calculated from the following equations [29]:

$$R_b = R_{conv} + R_{cond} + R_{grout} \quad (16)$$

$$R_{conv} = 0.5\, \frac{1}{\pi d_i h_i} \quad (17)$$

$$R_{cond} = 0.5\, \frac{\ln(d_o/d_i)}{2\pi k_{pipe}} \quad (18)$$

$$R_{grout} = \frac{1}{4\pi k_{grout}}\left[ln\left(\frac{r_b}{r_o}\right) + ln\left(\frac{r_b}{L_s}\right) + \frac{k_{grout}-k}{k_{grout}+k} \times ln\left(\frac{r_b^4}{r_b^4 - \left(\frac{L_s}{2}\right)^4}\right)\right] \quad (19)$$

where h_i is the convective heat transfer coefficient inside the tubes and can be calculated from *Dittus-Boelter* relation [30]:

$$h_i = \frac{Nuk_w}{d_i} = \frac{0.023Re^{0.8}Pr^m k_w}{d_i}$$
(20)

where, *m* is equal to 0.4 and 0.3 for the cases of heat absorption from the ground (in winter) and heat rejection to the ground (in summer) respectively.

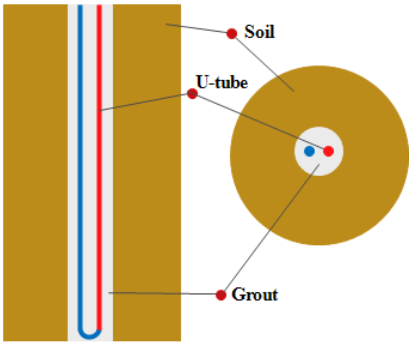

Fig. 2. *Schematic representation of a typical single U-tube ground heat exchanger*

The heat flux per unit length of the borehole is equal to the heat absorbed by the working fluid in the tubes and can be calculated from the following equations:

$$q' = \dot{m}C_p(T_{wo} - T_{wi})/L \quad (21)$$

Therefore by specifying the ground load and the design entering water temperature to the borehole, the leaving water temperature can be determined by Eq. (21).

D. Coefficient of Performance of Heat Pump

The operation of a heat pump is characterized by the *COP* defined as the ratio of the useful thermal energy and the energy consumed to obtain it [31]. For a heat pump in heating mode, *COP* can be calculated by the following equation:

$$\dot{Q}_H = \dot{Q}_L \frac{COP}{COP-1}$$
(22)

where $\dot{Q}_H$ is the heating capacity of the heat pump and $\dot{Q}_L$ is the absorbed heat in the evaporator. The difference between $\dot{Q}_H$ and $\dot{Q}_L$ is the input power to the heat pump (compressor power). The *COP* of a heat pump is a function of entering water temperature to its evaporator so the energy analysis of the GSHP is based on the instantaneous fluid temperature at the GHE outlet. This temperature defines the *COP* of the heat pump and hence the electricity consumption of it [5]. Manufacturers often provide *COP* versus temperature curves for heat pumps. Tarnawski and Leong [32] have presented the following equation to correlate the *COP* of any heat pump to its entering water temperature.

$$COP = COP_{baseline}(K_0 + K_1 T_{ewt} + K_2 T_{ewt}^2) \quad (23)$$

where T_{ewt} is the entering water temperature to the heat pump (water temperature at the GHE outlet), $COP_{baseline}$ is the nominal coefficient of performance of the heat pump which is provided by manufacturers and is measured at standard entering water temperature of 0°C. K_0, K_1 and K_2 are constant coefficients and are equal to 1, 0.0155970900 and 0.0001593100, respectively [32].

E. Solution Methodology

The design flowchart of geothermal radiant floor heating systems is shown in Fig. 3. As shown in this figure, first the structural and climatic characteristics of the building are specified, then a value of heat flux from the floor is guessed and the temperatures of the 6 lateral surfaces of the room and the internal air temperature are calculated from the system of 7 equations and 7 unknowns as discussed in section 2.1. At the next step, the mean radiant temperature and cloth temperature are calculated from Eqs. (8) and (11). Then the Predicted Mean Vote (PMV) index can be calculated from Eq. (10) for a seated person in the center of the room.

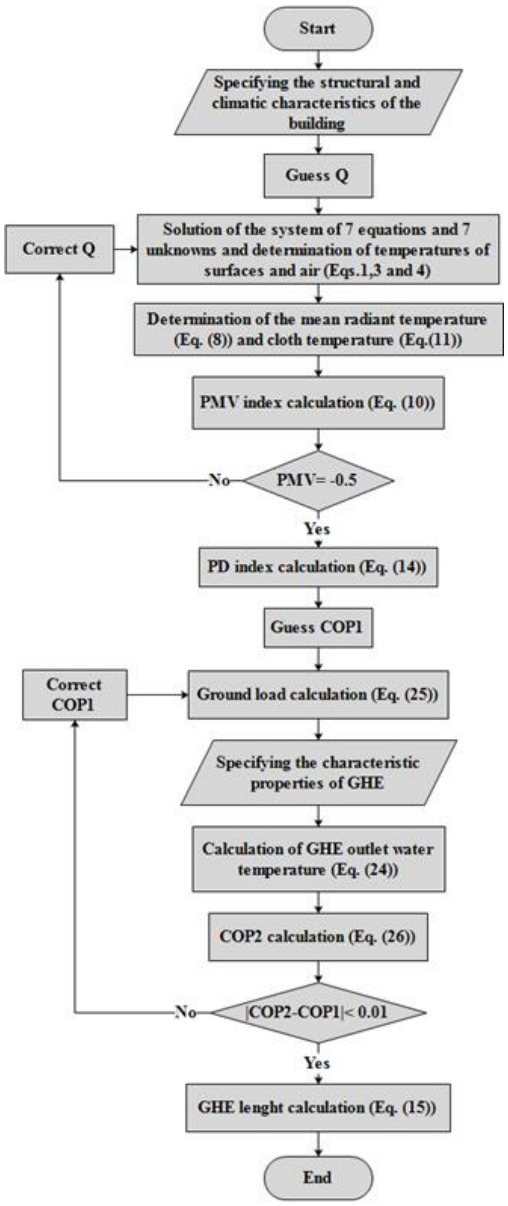

Fig. 3. *Solution flowchart for designing the combined GSHP-hydronic floor heating system*

If the PMV index value is close enough to -0.5, computations will be stopped and the considered value of the heat flux from the floor will be chosen as the final design heat flux from the floor, otherwise the value of the heat flux is corrected and the calculations will be continued. After calculation of required floor heat flux and temperatures of room air and internal room surfaces, the *PD* index can be calculated using Eq. (14).

In order to design the GHE, the floor heat flux is specified from the previous stage, then a value of *COP* for the heat pump is guessed and the ground load is calculated from Eq. (25). By specifying the characteristic properties of GHE, the extracted water temperature from the borehole can be determined by Eq. (24). As mentioned in the previous section, the *COP* of a GSHP is a function of the fluid temperature at the GHE outlet, so a new value of *COP* is determined based on this temperature (Eq. (26)). New and old values of *COP* are compared and if the difference between them is less than a specified error (0.01), the calculations will be stopped and the GHE length will be calculated from Eq. (15), otherwise the old value of *COP* is replaced by the new one and the calculations will be continued.

Design approach for conventional geothermal forced air systems is a little different. The design flowchart for these systems is shown in Fig. 4.

According to this figure, first the structural and climatic characteristics of the building are specified, and then a value for room air temperature is guessed. The value of mean radiant temperature is assumed equal to the air temperature [28] and the cloth temperature is determined by Eq. (11). Then the *PMV* index can be calculated from Eq. (10) for a seated person in the center of room. If the value of this index is close enough to -0.5, computations will be stopped and the guessed value of the air temperature will be chosen as the final air temperature in the room, otherwise the value of the guessed air temperature is corrected and the calculations will be continued. As the next step, the room heating load can be calculated by determining the heat losses from the walls and roof and also the heat loss due to infiltration. The method of designing the GHE in this case is similar to the procedure described for the geothermal radiant floor system.

Another difference between two described systems (floor heating and forced air) is the value of air velocity in the room which is considered equal to 0.1 m/s and 0.2 m/s for floor heating and convective systems, respectively [28]. A handmade computational program has been developed for the process of solution in accordance with the flowcharts.

F. *Model Validation*

The mathematical model was validated by comparing the predicted energy consumption of geothermal radiant floor and ceiling heating systems to data reported by Bojić et al. [22]. Present model predicted that the energy consumption of geothermal radiant ceiling panel is nearly 5.2% greater than radiant floor system that is in good agreement with the results reported in [22].

G. *Results and Discussion*

In the present work, the thermal performance of geothermal radiant floor heating system has been studied in terms of energy consumption and thermal comfort.

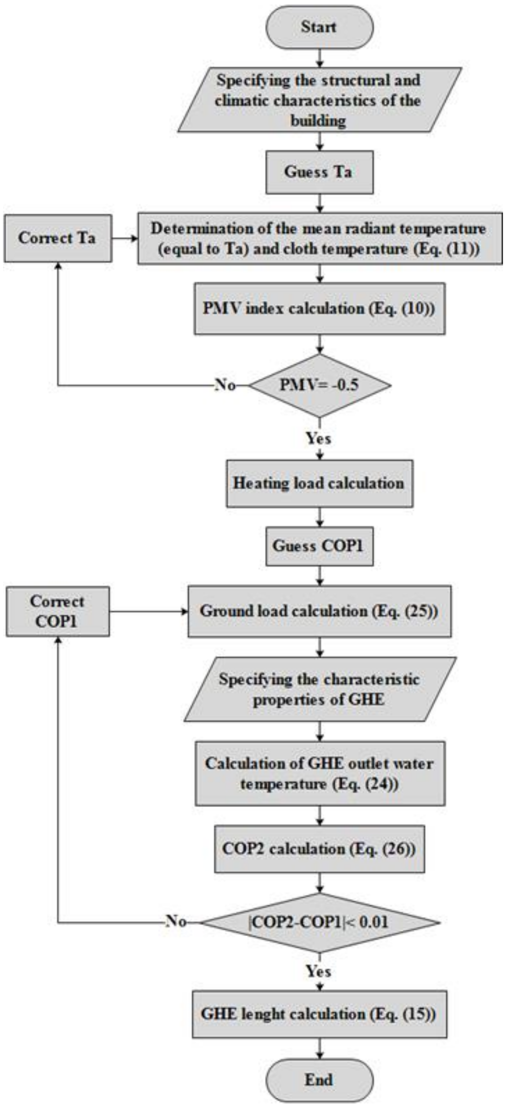

Fig. 4. *Solution flowchart for designing the conventional GSHP with convective distributor*

For this purpose, the performance of a GRFH has been calculated and compared with that of a GFA system for a 3×3×3 m^3 specified space in two cities with different climatic conditions of Iran. Cities of Tabriz, Tehran were chosen as representatives of cold and moderate climates of Iran. Since, the heating load of buildings plays a key role in design of ground heat exchanger in heating dominated regions and given that this factor depends on the construction and types of exterior walls, in this study four possible cases of exterior walls and roof have been considered for the room (see Fig. 5).

Walls are constructed of brick with the facade of travertine stone and the roof is considered joist-cement block. Some other required design data are listed in Table 2. The values of occupants' cloth resistance are considered equal to 0.7 clo and 1.0 clo [27] and the values of metabolic rate are considered equal to 1.0 Met and 1.2 Met for the cases of residential and official buildings, respectively [27].

The compressor power and the required GHE length of convective and radiant heating systems, for heating of residential and official buildings with different number of external walls and roof (Fig. 5), are calculated for three climatic conditions at the same level of thermal comfort (PMV≅-0.5). Results have been shown in Table 3. Percentage of reduction in the energy consumption and the required GHE length of the GRFH system in comparison to GFA system, are presented in Tables 4 and 5 respectively. The results show that the energy consumption and the required GHE length of the proposed system are about 12-18 % and 20-27 % lower compared to convective systems in the cases of residential and official buildings respectively.

For example, the compressor power of convective and radiant floor heating systems, for a residential building with one external wall and external roof, located in Tehran (as moderate climate), is 148 W and 126 W respectively. The required GHE length for same cases is 12.8 m and 10.9 m respectively.

The results show that for this case, the compressor power (energy consumption) and the required GHE length are approximately 15% lower for radiant floor heating system compared to convective system.

TABLE II. APPLICATION DATA

Property	Value
Grout thermal conductivity	1.5 W/mK
Soil thermal conductivity	1.4 W/mK
Soil density	1925 kg/m^3
Soil specific heat capacity	1400 J/kgK
Soil thermal diffusivity	0.52×10^{-6} m^2/s
Tube thermal conductivity	0.42 W/mK
Water thermal conductivity	0.582 W/mK
Water dynamic viscosity	1.442×10^{-3} kg/ms
Water specific heat capacity	4200 J/kgK
Water density	1000 kg/m^3
Water prandtl number	10.26
GHE tube inner diameter	0.025 m
GHE tube outer diameter	0.032 m
Borehole diameter	0.11 m
Water velocity in tubes	0.6 m/s
Nominal *COP* of heat pump	3.0
Undistributed ground temperature	Tabriz: 13 °C Tehran: 18 °C
Design entering water temperature to the borehole	Tabriz: 2 °C Tehran: 7 °C
Conductive resistance of walls	0.73 m^2K/W
Conductive resistance of roof	1.55 m^2K/W
Emissivity of walls and ceiling	0.95
Air velocity inside the room	Floor heating: 0.1 m/s Convective: 0.2 m/s
Convective heat transfer coefficient between the air and walls inside the room	10 W/m^2K
Convective heat transfer coefficient between the air and walls outside the room	50 W/m^2K
Cloth resistance	Residential: 0.7 clo Official: 1.0 clo
Metabolic rate	Residential: 1.0 Met

	Official: 1.2 Met

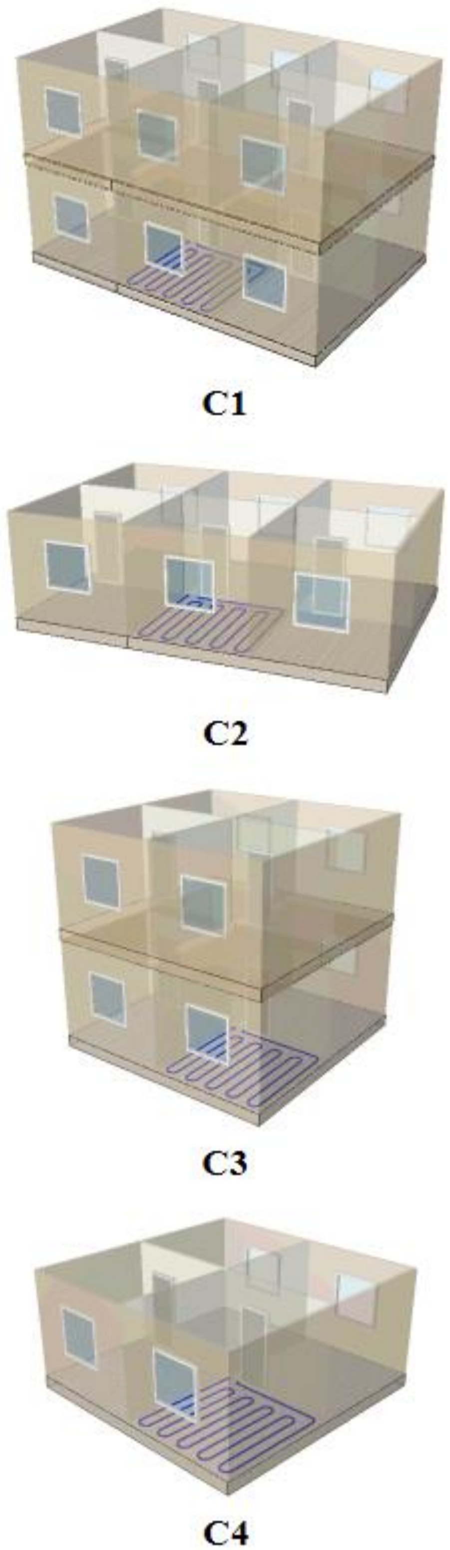

Fig. 5. *Four possible cases of exterior walls and roof of the specified space*

TABLE III. THE COMPRESSOR POWER (W) AND THE REQUIRED BOREHOLE LENGTH (M) FOR DIFFERENT CONSIDERED CASES

City (Climate)	Building Occupancy	Cases of external exposure walls and roof (Fig. 5)							
		C1		C2		C3		C4	
		Convective	Floor Heating	Convective	Floor Heating	Convective	Floor Heating	Convective	Floor Heating
Tabriz (Cold)	Residential	131 W 12.3 m	115 W 10.8 m	198 W 16.2 m	172 W 14.1 m	259 W 21.2 m	225 W 18.4 m	326 W 23.2 m	280 W 19.9 m

	Official	102 W 8.3 m	81 W 6.6 m	154 W 12.6 m	120 W 9.8 m	200 W 16.2 m	156 W 12.6 m	252 W 20.4 m	196 W 15.9 m
Tehran (Moderate)	Residential	98 W 8.8 m	84 W 7.6 m	148 W 12.8 m	126 W 10.9 m	194 W 17.5 m	165 W 14.9 m	244 W 22.1 m	205 W 18.6 m
	Official	76 W 6.5 m	59 W 5.0 m	115 W 9.9 m	88 W 7.6 m	150 W 12.9 m	114 W 9.7 m	189 W 16.2 m	143 W 12.2 m

TABLE IV. ENERGY SAVING BY USING 'GRFH' SYSTEM INSTEAD OF 'GFA' SYSTEM

City (Climate)	Building Occupancy	Energy Saving (%)			
		C1	C2	C3	C4
Tabriz (Cold)	Residential	12.2	13.1	13.1	14.1
	Official	20.6	22.0	22.0	22.2
Tehran (Moderate)	Residential	14.3	14.7	14.9	16.0
	Official	22.4	23.5	24.0	24.3

TABLE V. REDUCTION IN REQUIRED BOREHOLE LENGTH BY USING 'GRFH' SYSTEM INSTEAD OF 'GFA' SYSTEM

City (Climate)	Building Occupancy	Reduction of GHE size (%)			
		C1	C2	C3	C4
Tabriz (Cold)	Residential	12.2	13.0	13.2	14.0
	Official	20.5	22.2	22.2	22.1
Tehran (Moderate)	Residential	14.1	14.5	14.8	15.8
	Official	23.0	23.2	24.6	24.8

For the case of an official building, the compressor power is 115 W and 88 W and the required GHE length is 9.9 m and 7.6 m for convective and floor heating systems respectively. Therefore the energy consumption and the required GHE length are approximately 23% lower for the radiant floor heating system compared to convective system.

The calculation results are also shown in Figs. 6 to 9. It can be observed that by increasing the number of external walls (from C1 to C4) both the energy consumption and the required GHE (borehole) length will increase in all cases. It is because of the increased heat loss through the building envelope and therefore the increased heating load of the room. For example, in the case of a residential building in Tabriz, the compressor powers for floor heating system are 280 W and 115 W for C4 (two external walls and external roof) and C1 (one external wall) cases respectively. The increase in the energy consumption is about 143 % from C1 to C4 in this exampl e. Also

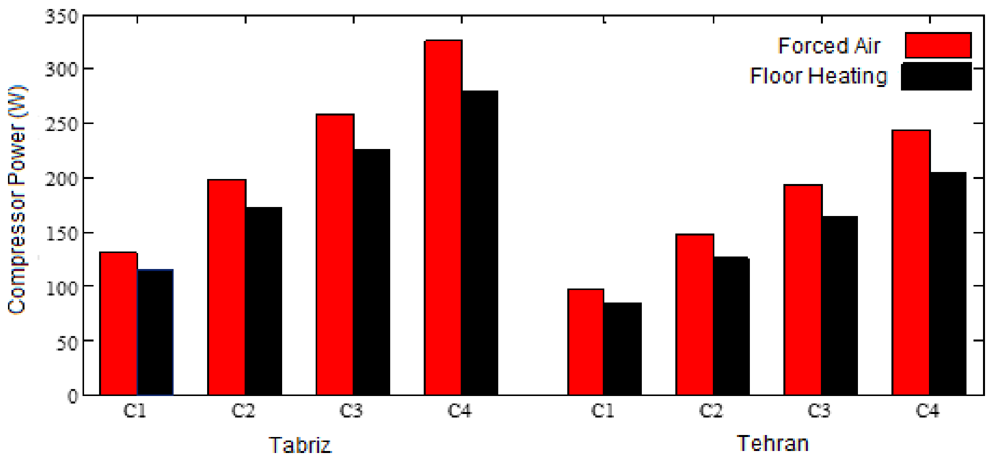

the increase in the required GHE size (borehole length) for the same conditions is about 84 %. Therefore the number of external walls can affect the energy consumption and the required GHE length of the system significantly and this means significant effect on both the capital cost and the operational cost of the system.

The climatic conditions can also be significant in the energy consumption and the required GHE size (borehole length). For example in the case of a residential building, the compressor powers for floor heating system are 131 W and 92 W for Tabriz and Tehran as cold and moderate climates, respectively.

H. Conclusion

In this study, the performance of geothermal hydronic radiant floor heating system is investigated in terms of the energy consumption and the thermal comfort. For this purpose, an analytical model has been developed to predict the performance of radiant floor heating system, ground source heat pump and underground vertical loop. Moreover the performance of the mentioned system has been compared to conventional geothermal forced air (convective) systems. Results demonstrate that at the same level of occupants thermal comfort, the energy consumption and the required borehole length of the combined geothermal and radiant floor heating system are about 12-18% and 20-27% lower compared to geothermal forced air (convective) system in the cases of residential and official buildings respectively. Results also indicate that the climatic conditions and type of building envelope are significant in energy consumption and the required borehole length.

Fig. 6. *Compressor power in residential building*

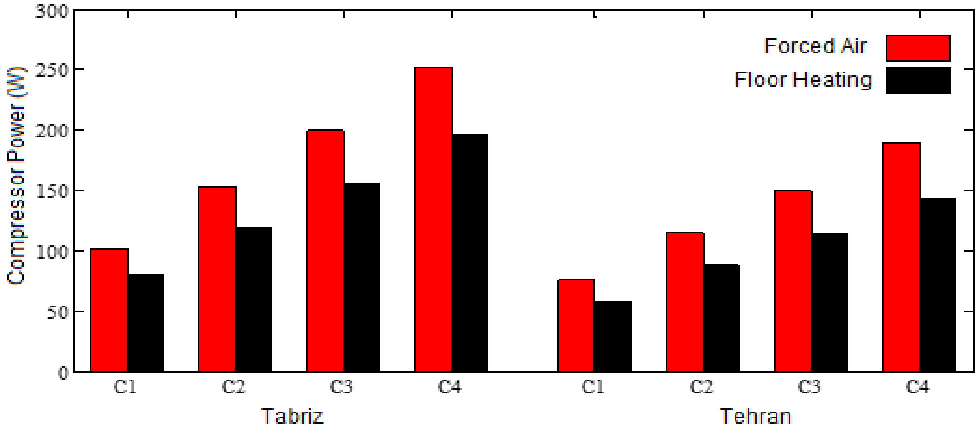

Fig. 7. *Compressor power in official building*

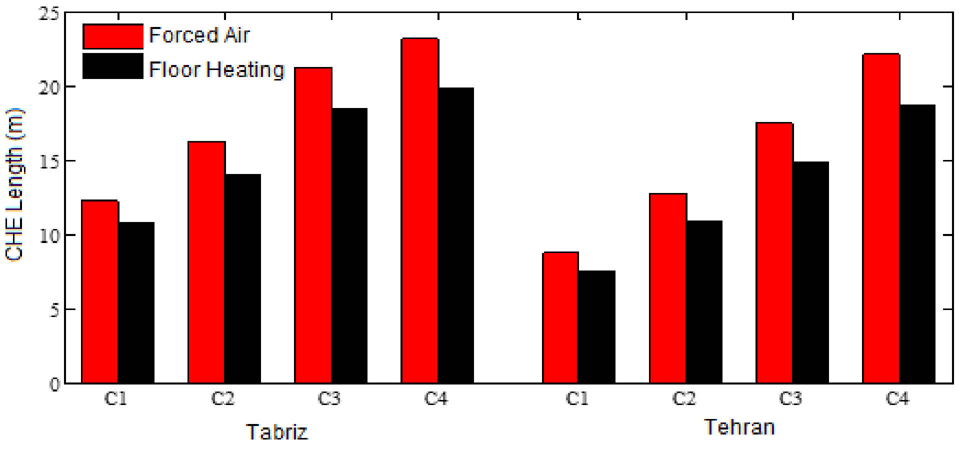

Fig. 8. *Ground heat exchanger (GHE) length in residential building*

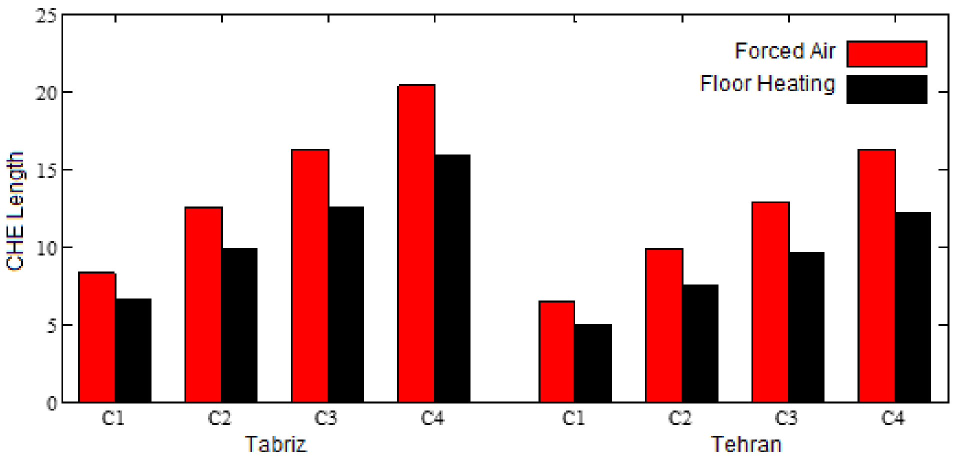

Fig. 9. *Ground heat exchanger (GHE) length in official building*

REFERENCES

[1] E. K. Akpinar and A. Hepbasli, "A comparative study on exergetic assessment of two ground-source (geothermal) heat pump systems for residential applications," Building and Environment, vol. 42, pp. 2004-2013, 2007.

[2] A. Hepbasli and M. Tolga Balta, "A study on modeling and performance assessment of a heat pump system for utilizing low temperature geothermal resources in buildings," Building and Environment, vol. 42, pp. 3747-3756, 2007.

[3] S. Liu, A. Shukla and Y. Zhang, "Investigations on the integration and acceptability of GSHP in the UK dwellings," Building and Environment, vol. 82, pp.442-449, 2014.

[4] H. Yang, P. Cui and Z. Fang, "Vertical-borehole ground-coupled heat pumps: A review of models and systems," Applied Energy, vol.87, pp. 16-27, 2010.

[5] I. Sarbu and C. Sebarchievici, "General review of ground-source heat pump systems for heating and cooling of buildings," Energy and Buildings, vol. 70, pp.441-454, 2014.

[6] A. Michopoulos and N. Kyriakis, "The influence of a vertical ground heat exchanger length on the electricity consumption of the heat pumps," Renewable Energy, vol. 35, pp.1403-1407, 2010.

[7] A. Casasso and R. Sethi, "Efficiency of closed loop geothermal heat pumps: A sensitivity analysis," Renewable Energy, vol. 62, pp.737-746, 2014.

[8] F. Michopoulos and N. Kyriakis, "Predicting the fluid temperature at the exit of the vertical ground heat exchangers," Applied Energy, vol. 86, pp. 2065-2070, 2009.

[9] S. P. Lohani and D. Schmidt, "Comparison of energy and exergy analysis of fossil plant, ground and air source heat pump building heating system," Renewable Energy, vol. 35, pp.1275-1282, 2010.

[10] X. Q. Zhai, M. Qu, X. Yu, Y. Yang and R. Z. Wang, "A review for the applications and integrated approaches of ground-coupled heat pump systems," Renewable and Sustainable Energy Reviews, vol. 15, pp. 3133-3140, 2011.

[11] L. I. Lubis, M. Kanoglu, I. Dincer and M. A. Rosen, "Thermodynamic analysis of a hybrid geothermal heat pump system," Geothermics, vol. 40, pp. 233-238, 2011.

[12] O. Ozgener and A. Hepbasli, "A parametrical study on the energetic and exergetic assessment of a solar assisted vertical ground-source heat pump system used for heating a greenhouse," Building and Environment, vol. 42, pp.11-24, 2007.

[13] O. Ozgener and A. Hepbasli, "Modeling and performance evaluation of ground source (geothermal) heat pump systems," Energy and Buildings, vol. 39, pp. 66-75, 2007.

[14] E. K. Akpinar and A. Hepbasli, "Comparative study on exergetic assessment of two ground-source (geothermal) heat pump systems for residential applications," Building and Environment, vol. 42, pp. 2004-2013, 2007.

[15] Y. Bi, X. Wang, Y. Liu, H. Zhang and L. Chen "Comprehensive exergy analysis of a ground-source heat pump system for both building heating and cooling modes," Applied Energy, vol. 86, pp.2560-2565, 2009.

[16] I. B. Kilkis, S. S. Sager and M. A. Uludag, "A simplified model for radiant heating and cooling panels," Simulation Practice and Theory, vol. 2, pp. 61-76, 1994.

[17] M. Rahimi and A. Sabernaeemi, “Experimental study of radiation and free convection in an enclosure with under-floor heating system,” Energy Conversion and Management, vol. 52, pp. 2752-2757, 2011.

[18] D. Zhang, N. Cai and Z. Wang, “Experimental and numerical analysis of lightweight radiant floor heating system,” Energy and Buildings, vol. 61, pp. 260-266, 2013.

[19] L. Fontana, “Thermal performance of radiant heating floors in furnished enclosed spaces,” Applied Thermal Engineering, vol. 31, pp. 1547-1555, 2011.

[20] M. Boji´c, D. Cvetkovi´c, V. Marjanovi´c, M. Blagojevi´c and Z. Djordjevi´c, “Performances of low temperature radiant heating systems,” Energy and Buildings, vol. 61, pp. 233-238, 2013.

[21] M. Rahimi and A. Sabernaeemi, “Experimental study of radiation and free convection in an enclosure with a radiant ceiling heating system,” Energy and Buildings, vol. 42, pp. 2077-2082, 2010.

[22] M. Bojić, D. Cvetković and L. Bojić, “Decreasing energy use and influence to environment by radiant panel heating using different energy sources,” Applied Energy, vol. 138, pp. 404-413, 2015.

[23] R. D. Watson and K. S. Chapman, Radiant heating & cooling handbook. New York: McGraw-Hill, 2004.

[24] J. P. Holman, Heat transfer, New York: McGraw-Hill, 1997.

[25] P. Q. Fanger, Thermal comfort analysis and application in environmental engineering, New York: McGraw-Hill, 1972.

[26] K. C. Parsons, Human thermal environments: The effects of hot, moderate, and cold environments on human health, comfort and performance, New York, Taylor & Francis, 2003.

[27] H. B. Awbi, Ventillation of buildings, New York, Taylor & Francis, 2003.

[28] E. Kjellsson, G. Hellstrom and B. Perers, “Optimization of systems with the combination of ground-source heat pump and solar collectors in dwellings,” Energy, vol. 35, pp. 26672673, 2010.

[29] M. Philippe and M. Bernier, Vertical Geothermal Borefields. ASHRAE Journal July 2010, pp. 20–29.

[30] L. Jun, Z. Xu, G. Jun and Y. Jie, “Evaluation of heat exchange rate of GHE in geothermal heat pump systems,” Renewable Energy, vol. 34, pp. 2898-2904, 2009.

[31] I. Sarbu and C. Sebarchievici, “General review of ground-source heat pump systems for heating and cooling of buildings,” Energy and Buildings, vol. 70, pp. 441-454, 2014.

[32] Natural Resources Canada. RET Screen engineering & cases textbook. Ground-source heat pump project analysis chapter [Online, 2013.01.10], http://www.retscreen.net/download.php/ang/479/0/Textbook_GSHP.pdf, 2013.